Molecular Microbiology (2001) **40**(3), 542–554

flp-1, the first representative of a new pilin gene subfamily, is required for non-specific adherence of *Actinobacillus actinomycetemcomitans*

Scott C. Kachlany,[1] Paul J. Planet,[1] Rob DeSalle,[2] Daniel H. Fine,[3] David H. Figurski[1] and Jeffrey B. Kaplan[3]*

[1]*Department of Microbiology, College of Physicians and Surgeons, Columbia University, New York, NY 10032, USA.*

[2]*Molecular Laboratories, American Museum of Natural History, New York, NY 10024, USA.*

[3]*Department of Oral Pathology, Biology, and Diagnostic Sciences, New Jersey Dental School, MSB Room C-636, 185 S. Orange Ave., Newark, NJ 07103, USA.*

Summary

***Actinobacillus actinomycetemcomitans*, a Gram-negative bacterium responsible for localized juvenile periodontitis and other infections such as endocarditis, produces long fibrils of bundled pili that are believed to mediate non-specific, tenacious adherence to surfaces. Previous investigations have implicated an abundant, small (≈6.5 kDa), fibril-associated protein (Flp/Fap) as the primary fibril subunit. Here, we report studies on fibril structure and on the function and evolution of Flp. High-resolution electron microscopy of adherent clinical strain CU1000N revealed long bundles of 5- to 7-nm-diameter pili, whose subunits appear to be arranged in a helical array similar to that observed for type IV pili in other bacteria. Fibrils were found to be associated with the bacterial cell surface and smaller structures thought to be membrane vesicles. A modified version of the CU1000N Flp1 polypeptide with the T7-TAG epitope fused to its C-terminus was expressed in the wild-type strain, and the presence of the modified Flp1 in fibrils was confirmed by immunogold electron microscopy with monoclonal antibody to T7-TAG. To determine the importance of Flp1 in fibril formation and cell adherence, we used transposon IS*903*φ*kan* to isolate insertion mutations in the *flp-1* gene (formerly designated *flp*). Mutants with insertions early in *flp-1* fail to produce fibrils and do not adhere to surfaces. Both fibril production and adherence were restored by cloned *flp-1 in trans*, thus providing the first evidence that *flp-1* is required for fibril formation and tight, non-specific adherence. One mutant was found to have an insertion near the 3′ end of *flp-1* that results in the expression of a truncated and altered C-terminus of Flp1. This mutant produced short, unbundled pili, and its adherence to surfaces was significantly less than that of wild-type bacteria. These findings and related observations with the Flp1-T7-TAG protein indicate that the C-terminus of Flp1 is important for the bundling and adherence properties of pili. Extensive sequence comparisons and phylogenetic analysis of 61 predicted prepilin genes of bacteria revealed *flp-1* to be a member of a novel and widespread subfamily of type IV prepilin genes. Thus, Flp pili are likely to be expressed by diverse bacterial species. Furthermore, we found that it is common for bacterial genomes to contain multiple alleles of *flp*-like genes, including the open reading frame (*flp-2*, previously designated *orfA*) immediately downstream of *flp-1* in *A. actinomycetemcomitans*. The duplication and divergence of *flp* genes in bacteria may be important to the diversification of the colonization properties of these organisms.**

Accepted 26 February, 2001. *For correspondence. E-mail kaplanjb@umdnj.edu; Tel. (+1) 973 972 5051; Fax (+1) 973 972 0045.

© 2001 Blackwell Science Ltd

Introduction

The ability of diverse bacteria to adhere to surfaces is a property important for the colonization of environmental niches and the production of biofilms (Costerton *et al*., 1995). Adherence is often mediated by proteinaceous appendages (pili, fimbriae) present on the bacterial cell surface (Klemm, 1994). Among the well-studied pilus systems are the P and type 1 pili of *Escherichia coli*, type 3 fimbriae of the Enterobacteriaceae, type IV pili of many Gram-negative bacteria, curli of *E. coli* and *Salmonella enteritidis* and CS1 pili of *E. coli* (Sauer *et al*., 2000). In general, the bacterial pilus is composed of a repeating polypeptide packed into a helical assembly. The tip of the bacterial pilus may display a protein adhesin that binds to host cells (Wizemann *et al*., 1999; Sauer *et al*., 2000). Because adherence to host surfaces is an early stage in bacterial infectious disease (Conway and Ronald, 1988; Hacker, 1992; Finlay and Falkow, 1997), pili biosynthesis and structure are considered to be promising targets for

Table 1. Strains and plasmids used in this study.

Strain or plasmid	Relevant characteristics	Reference
A. actinomycetemcomitans strains		
CU1000N	Spontaneous nalidixic acid-resistant mutant of rough clinical isolate CU1000	Kachlany *et al.* (2000b)
AA1649	CU1000N carrying pSK163	This work
JK1009	CU1000N *flp-1*Ω*1*::IS*903*φ*kan*; Km^r	This work
JK1010	CU1000N *flp-1*Ω*2*::IS*903*φ*kan*; Km^r	This work
JK1029	CU1000N *flp-1*Ω*3*::IS*903*φ*kan*; Km^r	This work
Plasmids		
pJAK16	Broad-host-range, mobilizable IncQ vector derived from pMMB67; Cm^r, *tac* promoter, $lacI^q$	Thomson *et al.* (1999)
pRA33	pJAK16 with *flp-1* of CU1000N expressed from *tac* promoter	This work
pSK163	pJAK16 with φ[*flp-1-T7Tag*] expressed from *tac* promoter	This work
pVJT128	IncQ plasmid vector with inducible, cryptic IS*903*φ*kan* for generating insertion mutations; Cm^r	Thomson *et al.* (1999)

medical intervention (Sprunt and Leidy, 1988; Sun *et al.*, 1990; Wizemann *et al.*, 1999).

Actinobacillus actinomycetemcomitans is a Gram-negative coccobacillus responsible for localized juvenile periodontitis and other systemic infections (Meyer and Fives-Taylor, 1998; Slots and Ting, 1999; Fives-Taylor *et al.*, 2000). The bacterium produces several potential virulence factors, including a leucotoxin (Kolodrubetz *et al.*, 1989; Lally *et al.*, 1989; Kachlany *et al.*, 2000a), cytolethal distending toxin (Meyer and Fives-Taylor, 1998; Shenker *et al.*, 1999) and iron- and haemin-binding proteins (Graber *et al.*, 1998). Fresh clinical isolates are able to adhere tightly to a variety of abiotic solid surfaces to form a tenacious biofilm (Fine *et al.*, 1999a; Kachlany *et al.*, 2000b). This remarkable property is thought to be important for colonization of the tooth surface by *A. actinomycetemcomitans* (Fine *et al.*, 1999b; Kachlany *et al.*, 2000b). Electron microscopy has revealed that these cells express long, thick fibrils composed of bundles of thin pili on their surface (Holt *et al.*, 1980; Scannapieco *et al.*, 1987; Rosan *et al.*, 1988; Fine *et al.*, 1999a, b). On solid medium, clinical isolates exhibit a rough colony morphology (Inouye *et al.*, 1990). The adherent clinical isolates can spontaneously give rise to non-adherent variants that lack fibrils and form smooth colonies on solid medium (Fine *et al.*, 1999b).

Biochemical studies have indicated that the pili of *A. actinomycetemcomitans* are likely to be composed of a 6.5 kDa protein designated Flp (fimbrial low-molecular-weight protein) (Inoue *et al.*, 1998). This protein was found to be associated in abundance with purified fibrils (Inoue *et al.*, 1998). Earlier studies indicated a 54 kDa protein (Fup) as a pilus subunit (Harano *et al.*, 1995), and protein sequence analysis of purified fibril preparations revealed an N-terminal amino acid sequence, presumed to be part of the 54 kDa fibril-associated polypeptide (Harano *et al.*, 1995), but later determined to be that of a low-molecular-weight protein, termed Fap (Ishihara *et al.*, 1997). Inoue *et al.* (1998) showed that Flp and Fap are the same protein and proposed that this protein was the major structural component of *A. actinomycetemcomitans* fibrils. Because of the presence of a second *flp* allele in *A. actinomycetemcomitans* (this work), we have designated the coding region for this protein as *flp-1*. The predicted polypeptide product of *flp-1* (Flp1) has a putative secretion signal peptide at its N-terminus that is cleaved upon export from the bacterial cell (Inoue *et al.*, 1998), and recent studies have shown that the C-terminal portion of the mature Flp1 protein is modified (Inoue *et al.*, 2000).

Recently, we identified seven *tad* genes (*tadABC-DEFG*) of *A. actinomycetemcomitans* that are required for tight non-specific adherence of the bacteria to surfaces (Kachlany *et al.*, 2000b). Non-polar mutations in any of the *tad* genes resulted in a defect in adherence and failure to produce fibrils, further strengthening the correlation between fibrils and adherence. The *flp-1* gene of *A. actinomycetemcomitans* is located upstream of the *tadABCDEFG* locus (Haase *et al.*, 1999; Kachlany *et al.*, 2000b), and we have predicted that the Tad proteins are involved in the assembly and secretion of Flp1 to form the long bundled fibrils of *A. actinomycetemcomitans*. Recently, Skerker and Shapiro (2000) described a putative *flp-1* homologue in *Caulobacter crescentus* and found that disruption of the gene abolished the ability to produce pili. In this report, we show that Flp1 of *A. actinomycetemcomitans* is required for both fibril formation and tight non-specific adherence of the bacteria to surfaces. In addition, modification of the C-terminus of Flp1 altered pili bundling and the adherence properties of *A. actinomycetemcomitans*. Extensive database searches revealed that a wide variety of bacteria encode genes whose predicted polypeptide products have remarkably high sequence similarity to Flp1. We used parsimony analysis to infer the evolutionary history of type IV prepilins and demonstrate that *A. actinomycetemcomitans flp-1* and its closest relatives form a novel and distinct subfamily of prepilin genes. The widespread

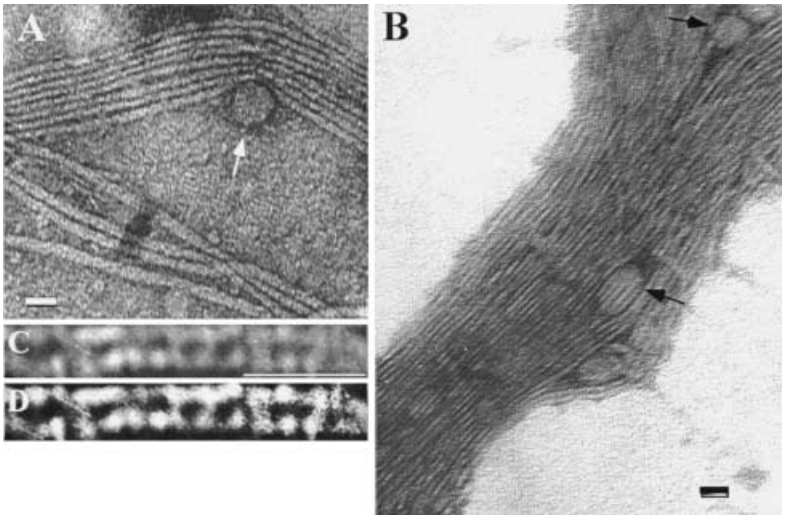

Fig. 1. High-resolution images of *A. actinomycetemcomitans* CU1000N fibrils. The bacteria were grown and prepared for electron microscopy as described in *Experimental procedures*.
A and B. Fibrils composed of bundled, individual pili. Arrows indicate the probable lipid vesicles.
C. High-magnification image of an individual fibril showing the putative helical assembly.
D. High-contrast image of (C).
Scale bars in (A) and (B) represent 20 nm; (C) 10 nm.

occurrence of *flp* subfamily genes suggests that Flp pili are expressed by a broad range of bacterial species.

Results

High-resolution electron microscopy of A. actinomycetemcomitans *fibrils*

Cells of the rough, adherent clinical isolate CU1000N were examined by high-resolution transmission electron microscopy at high magnifications ($> \times$ 200 000). As reported previously for this strain (Kachlany *et al*., 2000b), the cells were associated with numerous, long, bundled fibrils consisting of large parallel arrays of thin fibrils or pili (Fig. 1). Individual pili were rarely observed. We determined the diameter of the pili to be 5–7 nm (Fig. 1). Image analysis of high-magnification images of single pili (Fig. 1C and D) revealed a regular structure resembling the helical stacking of subunits observed for other pili (Sauer *et al*., 2000).

The bundled fibrils were tightly associated with cells because they remained attached even after vigorous washing, for example during the immunogold labelling procedure (see below). Fibrils were often observed to be associated with more than one cell. This property very likely accounts for the autoaggregation property of wild-type *A. actinomycetemcomitans*, which is also correlated with the presence of fibrils (Kachlany *et al*., 2000b). However, we never observed fibrils or pili anchored in the cell membrane or localized to a particular part of the cell, such as a pole, and we were unable to detect potential sites of insertion into the cell, such as indentations or pinching of the membranes at points of contact. One possible explanation is that the cells release the pili into the extracellular milieu and then bind to them. Structures appearing as lipid blebs or vesicles (arrows) were commonly associated with and entangled in the large bundles of pili (Fig. 1A and B). Others have observed that membrane vesicles are usually associated with *A. actinomycetemcomitans* cells, but the role of these vesicles in the biology of *A. actinomycetemcomitans* has not yet been determined. Nevertheless, it is clear that the pili not only interact in parallel arrays to form thick fibres, but also adhere to environmental surfaces, *A. actinomycetemcomitans* bacterial cells (Kachlany *et al*., 2000b) and membrane vesicles.

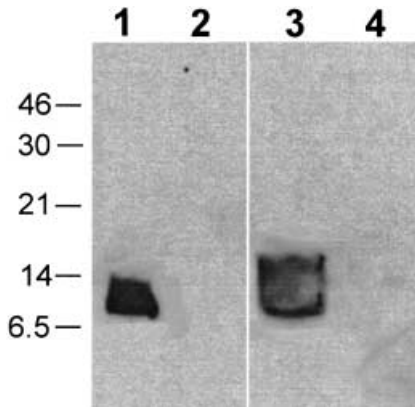

Fig. 2. Expression and detection of Flp1-T7 polypeptide in *A. actinomycetemcomitans* CU1000N. Cells were grown in the presence of 1.0 mM IPTG as described. Either whole cells (lanes 1 and 2) or supernatants (lanes 3 and 4) were loaded onto a 20% resolving polyacrylamide gel. Samples are CU1000N harbouring pSK163 (lanes 1 and 3) or control plasmid pJAK16 (lanes 2 and 4). The diffuse band is consistently seen and is possibly caused by modification of the protein, as suggested by Inoue *et al*. (2000).

Flp1-T7 localizes to A. actinomycetemcomitans *fibrils*

To confirm that *flp-1* does indeed encode a protein that is part of the fibrils, we constructed a gene fusion that

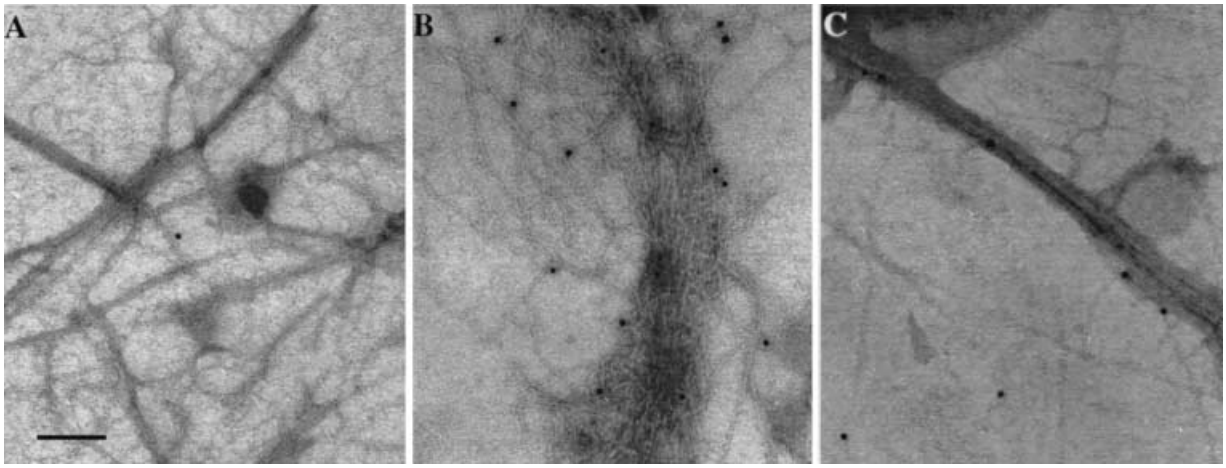

Fig. 3. Immunoelectron localization of Flp1-T7 to *A. actinomycetemcomitans* CU1000N fibrils. The bacteria were grown and prepared for immunogold electron microscopy as described in *Experimental procedures*.
A. Fibrils produced by the control strain containing the plasmid vector.
B and C. Fibrils produced by CU1000N strain expressing Flp1-T7. Gold-conjugated antibody (10 nm) recognizing Flp1-T7 is evident as electron-dense particles along the fibrils. Particles on grids with control cells (A) were extremely rare. Scale bar represents 100 nm for all frames.

allowed the expression of an Flp1 polypeptide fused with the 11-amino-acid T7-TAG at its C-terminus (designated Flp1-T7). This fusion was inserted downstream of the IPTG-inducible *tac* promoter in a broad-host-range IncQ plasmid vector and mobilized by conjugative transfer into the rough, adherent *A. actinomycetemcomitans* strain CU1000N. Induction of the *tac* promoter with IPTG led to the expression of a single polypeptide species of the expected mass of 7.5 kDa in whole cells and culture supernatants, as determined by Western blot analysis with monoclonal antibody specific for T7-TAG (Fig. 2). These cells, expressing both Flp1-T7 polypeptide and wild-type Flp1, were found to adhere to surfaces, although

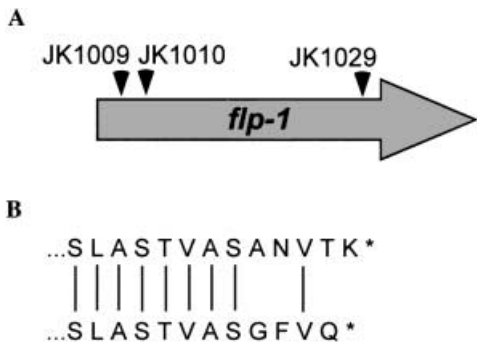

Fig. 4. Location of transposon insertions in the *flp-1* mutants.A. The arrow signifies *flp-1* from CU1000N. Insertion sites for the three mutants are indicated by arrows. The nucleotide numbers after which the insertions are located in the gene are as follows: JK1009, 16; JK1010, 18; JK1029, 203.B. The amino acid sequences of the C-terminal regions of wild-type Flp1 (top) and the predicted polypeptide product expressed by JK1029 (bottom). The asterisks mark the C-terminal residues, and the vertical lines indicate identical amino acids.

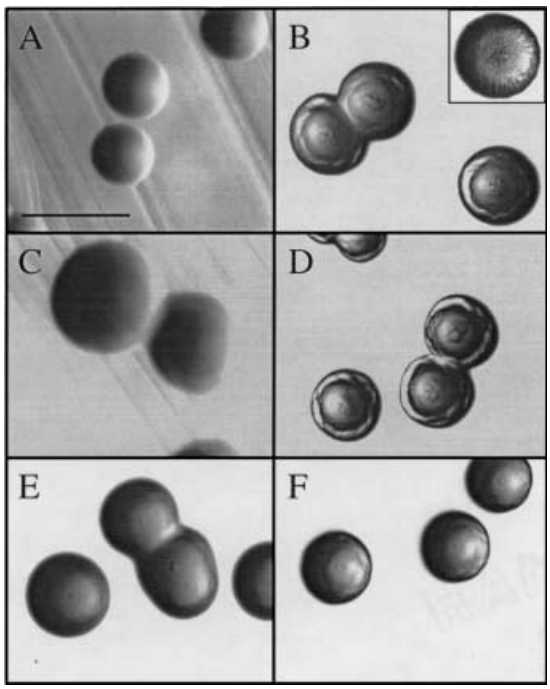

Fig. 5. Colony morphology of *flp-1* mutants. Strains were grown on AAGM-Cm agar containing 1 mM IPTG. Shown on the left are colonies from mutant strains carrying plasmid vector (pJAK16): (A) JK1009; (C) JK1010; (E) JK1029. On the right are colonies from mutant strains carrying the *flp-1* $^{+}$ plasmid pRA33: (B) JK1009; (D) JK1010; (F) JK1029. The insert in (B) is the clinical rough strain CU1000N on AAGM. Roughness was not completely restored in the complemented JK1009 and JK1010 mutants probably because of non-stoichiometric amounts of the plasmid-borne *flp-1*. Scale bar represents 1.0 mm for all frames.

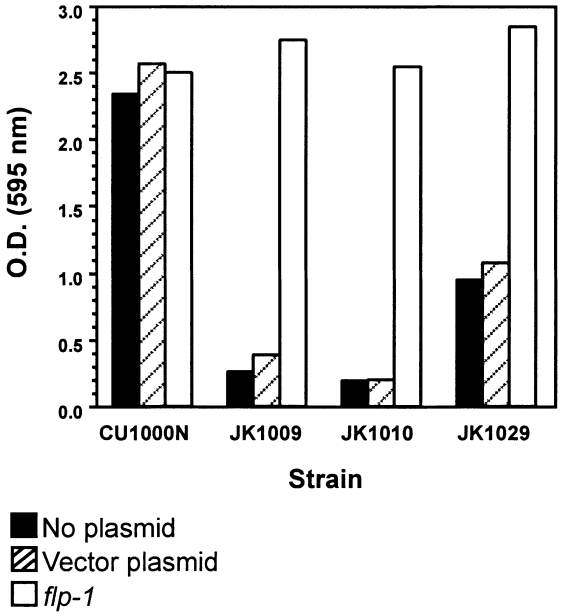

Fig. 6. Relative adherence of *A. actinomycetemcomitans* strains to polystyrene e plates. The adherence of wild-type CU1000N and *flp-1* mutant strains JK1009, JK1010 and JK1029 was assessed by the semi-quantitative colorimetric adherence assay described in *Experimental procedures*. In this assay, adherence is proportional to OD values measured at 595 nm. For each strain, black bars indicate strains lacking plasmid; hatched bars, strains harbouring plasmid vector pJAK16; and open bars, strains carrying the *flp-1*$^+$ plasmid pRA33.

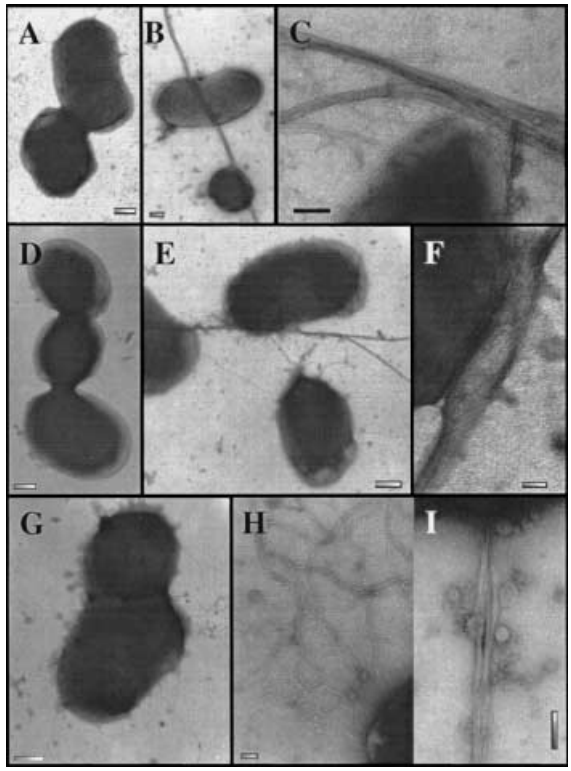

Fig. 7. Fibril production by *flp-1* mutants. Strains were grown and prepared for examination by electron microscopy after negative staining with uranyl acetate as described in *Experimental procedures*. Top row, mutant JK1009 containing plasmid vector (A) or *flp-1*$^+$ plasmid pRA33 (B and C). Middle row, JK1010 containing plasmid vector (D) or *flp-1*$^+$ plasmid pRA33 (E and F). Bottom row, JK1029 containing plasmid vector (G) or *flp-1*$^+$ plasmid pRA33 (H and I). Scale bars: 200 nm (A, B, D, E and G), 100 nm (C and I) and 50 nm (F and H).

less well than wild-type cells (data not shown), and produce fibrils. Immunogold electron microscopy was then used to test for the presence of Flp1-T7 in fibrils. The bacteria were induced with IPTG, then treated with primary anti-T7-TAG monoclonal antibody and secondary colloidal gold-labelled antibody and examined. Flp1-T7 was found to co-localize with the fibrils of CU1000N (Fig. 3B and C), in contrast to results with the control strain of CU1000N containing the vector plasmid (Fig. 3A). These results demonstrate that Flp1-T7 is secreted and associated with fibrils.

Fig. 8. Identification of the *flp* subfamily of type IV prepilin genes. The phylogenetic tree of the type IV prepilin superfamily was produced by a maximum parsimony-based algorithm as described in *Experimental procedures*. The two major families, IVA and IVB, are denoted by coloured boxes. The *flp* subfamily is designated by a vertical line. Numbers on branches denote support indices for the tree (see *Experimental procedures*). The first number annotated with a 'd' is the Bremer index for the node at the end of that branch. The second number, after the slash, is the bootstrap value. Only bootstrap values $>$ 50% are shown. Accession numbers for the genes and loci represented in this tree are as follows: *Acinetobacter* sp. BD413(*comP*, AAC45886.1); *Actinobacillus actinomycetemcomitans* (*pilA*, AAF89188.1|AF268318; *flp-2* BAA25887.1; *flp-1* BAA25886.1); *Aeromonas hydrophila* (*tapA*, AAC43995.1); *Aeromonas salmonicida* (*tapA*, AAC23566.1); *Azoarcus* sp. BH72(*pilA*, AAC27898.1); *Bacillus anthracis* (pX01–64, AAD32368.1|AAD32368; pX0163, AAD32367.1); *Bradyrhizobium japonicum* (*flp* from sequence fragment BJU79771); *Chlorobium limicola* (*flp-1* and *flp-2* come from the fully sequenced plasmid pCL1 CLU77780); CollB-P9(*pilS*, BAA31138.1); *Dichelobacter nodosus* (*fimA*, CAA36648.1); *Eikenella corrodens* (ecpB, CAA78251.1; ecpA, CAA78250.1); *Escherichia coli* (*ppdD,* AAC36923.1; *lngA*, AAC33154.1; bfpA, AAC44040.1); *Haemophilus influenzae* (*ppdD*, AAC21963.1); *Klebsiella denitrificans* (*kdpA*, AAB48592.1; kdpB, AAB48593.1; *kdpC*, AAB48595.1; *kdpD*, AAB48594.1); *Moraxella bovis* (pilin, AAA53087.1); *Neisseria gonorrhoeae* (*pilE*, AAC38435.1); *Neisseria meningitidis* (*pilE*, CAA89972.1); *Pasteurella multocida* (*ptfA* AAF61196.1/AF154834); *Pseudomonas aeruginosa* (pilin, AAC60461.1; type IV pilin-2, AAC41410.1; type IV pilin-1, AAC63062.1); *P. aeruginosa* PAO1(propilin, AAA25954.1; *flp*, AAG07694.1|AE004847-1 PA4306); *Pseudomonas stutzeri* (*pilA-2*, CAB60735.1; *pilA-1*, CAB60734.1); *Pseudomonas syringae* (prepilin, AAA25974.1); R64(*pilS*, BAA77979.1); R721(PilS, BAB12642.1); *Salmonella enterica* ssp. *dublin* (*pilS*, AAF81215.1|AF247502); *Salmonella enterica* ssp. *typhi* (*pilS*, AAC98887.1); *Salmonella enterica* ssp. *typhimurium* (*ppdD* CAB89833.1); *Synechocystis* PCC6308(*hofG-1* BAA17750.1; *hofG-2* BAA17751.1; *hofG-3* BAA18656.1); *Vibrio cholerae* (fimbrial protein VC2423, AAF95566.1; *tcpA*, P23024); *Xanthomonas campestris* (*fimB*, CAA88681.1; *fimA*, CAA88680.1). All other ORFs were found in searches of unannotated genomes and were named according to their phylogenetic grouping. When more than one *flp* gene is present in a given organism, the gene is designated by an allele number.

Isolation and characterization of flp-1 *mutants*

To determine whether Flp1 is required for fibril formation and/or the tight adherence of *A. actinomycetemcomitans*, we isolated transposon IS*903*ϕ*kan* insertion mutants that interrupt the *flp-1* gene of the rough, adherent strain CU1000N. Because non-adherent mutants of *A. actinomycetemcomitans* were found to display a smooth colony phenotype (Kachlany *et al*., 2000b), we picked smooth-appearing colonies after transposon mutagenesis, as

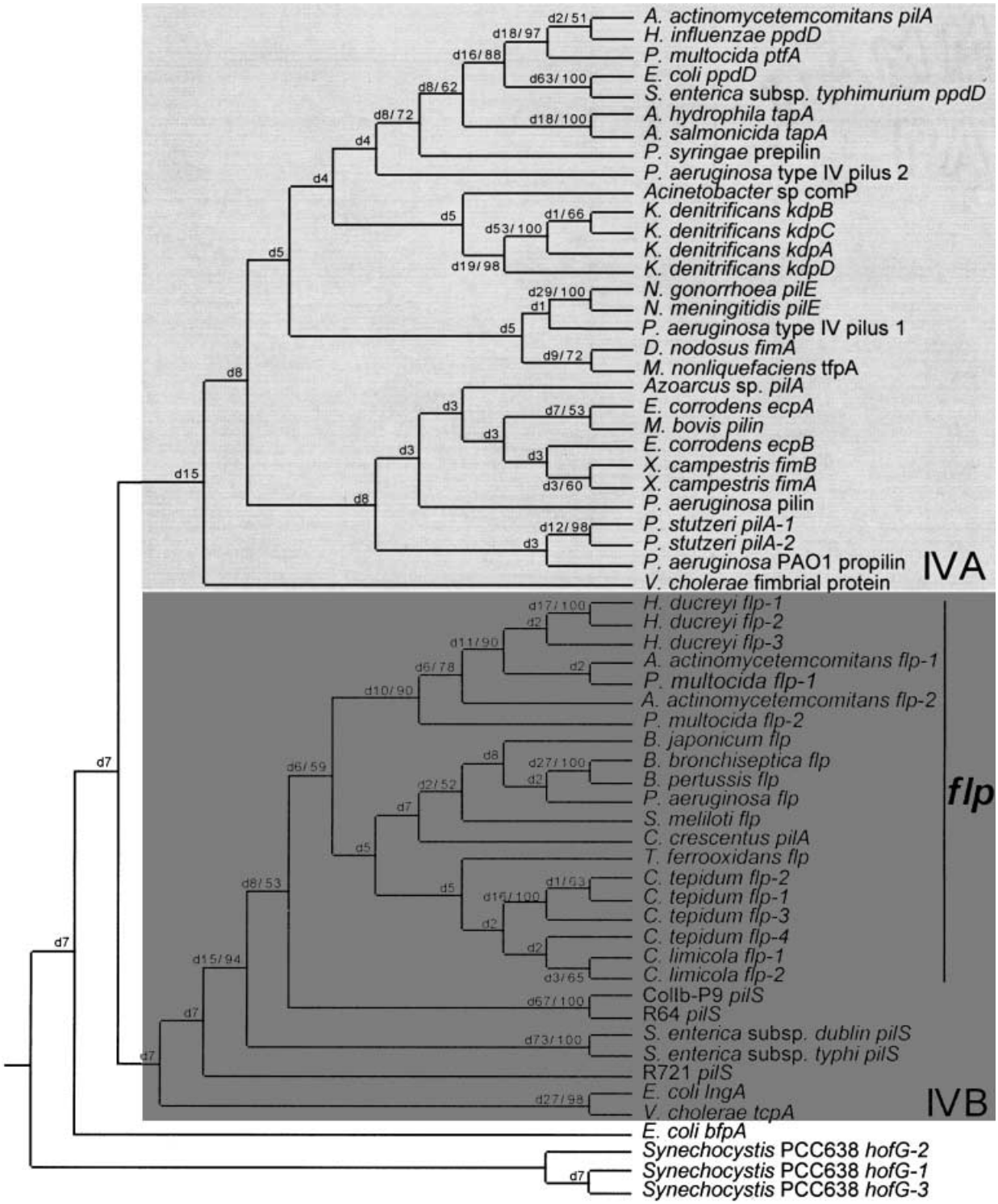

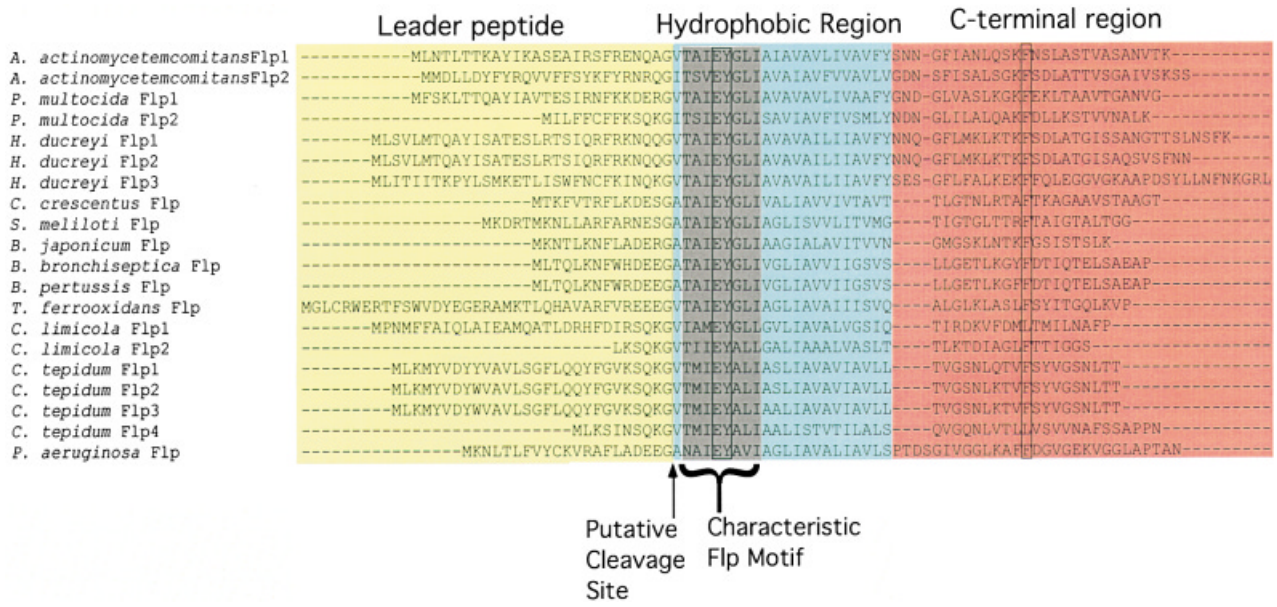

Fig. 9. Alignment of the predicted products of *flp* subfamily members. Three-domain structure is shown by coloured boxes (yellow, leader peptide; blue, hydrophobic region; red, variable C-terminus). The grey box shows the area of highest conservation between Flp proteins. Note the absolute conservation of the adjacent glutamate and tyrosine residues (boxed). Within the C-terminal region, a phenylalanine residue is conserved in all but two examples (*C. limicola* Flp1 and *P. aeruginosa* Flp1). The predicted polypeptide products of *flp-1* and *flp-2* of the clinical isolate CU1000N are slightly different from those of strain 304a (Inoue *et al*., 1998). The Flp1 polypeptides differ at two positions and the Flp2 polypeptides at four positions.

described in *Experimental procedures*. The mutants were screened further by polymerase chain reaction (PCR) for transposon insertions within *flp-1*, and candidates were sequenced to map the insertion sites.

We isolated three independent mutants with disruptions of *flp-1* (Fig. 4A). The transposon insertions in JK1009 and JK1010 are located at the 5′ end of *flp-1*, within the coding region for the putative N-terminal signal sequence. Both JK1009 and JK1010 exhibit a smooth colony phenotype on solid medium (Fig. 5A and C), and both are completely defective in adherence (Fig. 6). Expression plasmids containing the wild-type *flp-1* gene cloned downstream of the IPTG-inducible *tac* promoter were introduced into the mutants. Upon addition of IPTG to the cells, wild-type *flp-1 in trans* restored adherence and caused colonies to appear rougher. The transposon insertion in the third mutant, JK1029, is located at the 3′ end of *flp-1*, which alters only the terminal five amino acids of the polypeptide product (Fig. 4B). In contrast to the smooth colony phenotypes of JK1009 and JK1010, JK1029 colonies exhibit internal dimples reminiscent of the star-like centres of wild-type, rough colonies (Fig. 5F). In addition, broth cultures of JK1029 displayed a partial adherence phenotype (Fig. 6). Expression of wild-type *flp-1 in trans* in JK1029 increased adherence. However, unlike complemented JK1009 and JK1010, gentle mixing caused cells of complemented JK1029 to be removed from the wall of the tube. In addition, *flp-1* did not alter the colony phenotype of JK1029 (Fig. 5F), indicating a possible dominant-negative phenotype caused by expression of the truncated Flp1 in JK1029.

Next, we examined the *flp-1* mutants for the presence of fibrils (Fig. 7). Both non-adherent mutants, JK1009 and JK1010, completely lacked bundled fibrils (Fig. 7A and D), and the presence of wild-type *flp-1 in trans* restored the expression of fibrils (Fig. 7B, C, E and F). Interestingly, JK1029 produced fibrils (Fig. 7G), but they appeared as short, individual pili, in contrast to the long, bundled fibrils of the wild-type strain (Fig. 1). Upon complementation of JK1029 mutation with wild-type *flp-1*, the fibrils appeared longer and displayed bundling, albeit to a lesser extent than those of the complemented JK1009 and JK1010 strains (Fig. 7H and I).

From these results, we conclude that *flp-1* is required for the formation of fibrils and for the tight adherence of *A. actinomycetemcomitans* to surfaces.

Construction of a gene tree for prepilins

From searches of public databases, we selected 61 putative prepilin genes that met our criteria for inclusion in this analysis (see *Experimental procedures*). Using a maximum parsimony-based algorithm, we reconstructed a phylogenetic tree depicting the relationships of putative prepilin genes (Fig. 8). Because almost all the predicted polypeptide sequences are significantly shorter than 150

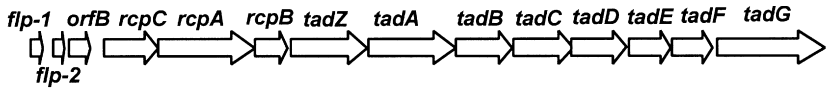

Fig. 10. Arrangement of genes in the *flp–rcp–tad* region of the *A. actinomycetemcomitans* CU1000N genome. Shown are genes and ORFs in the 12 kb region flanked by *flp-1* and *tadG*. The *rcp* (Haase *et al*., 1999) and *tad* genes (Kachlany *et al*., 2000b) have been described elsewhere. The second *flp* allele, *flp*-2, was previously referred to as *orfA* (Inoue *et al*., 1998). Mutations in *tadZ* cause loss of tight, non-specific adherence of *A. actinomycetemcomitans* (P. Planet, unpublished results).

amino acids in length, we combined amino acid and nucleotide sequence data in the same matrix for phylogenetic analysis. This technique allows efficient extraction of sequence data by weighting data according to the genetic code and adding robustness to phylogenetic inference (Agosti *et al*., 1995). Combining DNA and amino acid data successfully resolved all gene relationships in the tree, whereas a tree constructed using amino acid data alone (data not shown) left many relationships unresolved. Bremer indices and bootstrap supports were used to assess confidence in the relationships represented on the tree (Felsenstein, 1985; Bremer, 1995). Although a number of nodes, albeit mostly basal nodes, were not well supported by the bootstrap percentages owing to the short lengths of the sequences, the Bremer indices strongly supported the most parsimonious phylogeny (Fig. 8).

Two distinct gene families could be distinguished within the type IV prepilin gene phylogeny. One large monophyletic clade contains genes previously classified by other criteria as type IVA prepilin genes, such as *Pseudomonas aeruginosa pilA and E. coli fimA* (Strom and Lory, 1993). A second large group contains almost all the prepilin genes previously designated as type IVB, including *Vibrio cholerae tcpA*, *Salmonella* spp. *pilS* and *A. actinomycetemcomitans flp-1* (Strom and Lory, 1993; Skerker and Shapiro, 2000). One gene previously classified in the type IVB group, *E. coli bfpA* (Strom and Lory, 1993), falls outside both families. This phylogenetic classification suggests that *bfpA* is the descendent of a lineage that diverged from the prepilin ancestral trunk before the IVA and IVB families split. Therefore, its previous classification as a type IVB prepilin may reflect the retention of ancestral traits in the IVB family. Although Bremer decay indices strongly support this exclusion of *bfpA*, it is not well supported by bootstrap values. Therefore, the location of *bfpA* in the type IV prepilin superfamily is still tentative.

Identification of a distinct flp *subfamily of prepilin genes*

Further analysis of the type IVB family allowed us to discern a distinct *flp* subfamily of prepilin genes (Fig. 8). The genes of the *flp* subfamily have several distinguishing features. First, the predicted polypeptide products of all *flp* subfamily genes range from 50 to 80 amino acids (Fig. 9), whereas other type IV prepilins generally exceed 120 amino acids. In addition, alignment of the *flp* subfamily polypeptide products revealed a shared motif ('Flp motif'; Fig. 9) at the N-terminus of the predicted mature peptide. This motif is characterized by adjacent glutamate and tyrosine residues in its centre, and it occurs within a stretch of $\approx$20 hydrophobic, non-polar, aliphatic amino acids. Thirdly, the predicted polypeptides usually contain a phenylalanine residue close to the middle of their hydrophilic C-terminal domains.

Other important distinguishing features of the *flp* subfamily are related to the genomic loci that contain the genes. We found that all known genes of the *flp* subfamily occur in clusters of putative genes that are similar to those in the *flp–rcp–tad* locus of *A. actinomycetemcomitans* (Fig. 10) (Haase *et al*., 1999; Kachlany *et al*., 2000b). No other type IV prepilins in this phylogeny are associated with similar gene clusters. As we have shown here for *flp-1*, the *tadABCDEFG* genes are also required for tight adherence and fibril formation in *A. actinomycetemcomitans* (Kachlany *et al*., 2000b). We proposed previously that the Tad proteins are components of the machinery involved in the assembly and secretion of fibrils (Kachlany *et al*., 2000b). Thus, Flp is likely to be the substrate for this machinery.

We found that *flp*-encoding genomes commonly possess more than one closely linked *flp* allele. Indeed, the genomes of *Haemophilus ducreyi*, *Pasteurella multocida* and *Chlorobium tepidum* contain three or more clustered *flp* alleles. Our analysis also revealed a duplicated *flp* allele in *A. actinomycetemcomitans*. This second putative gene, previously designated *orfA*, is located immediately downstream of *flp-1*. We have therefore designated this allele as *flp-2* (Figs 9 and 10). We are currently investigating the possibility that *A. actinomycetemcomitans flp-2* also functions in adherence and/or the production of fibrils.

Discussion

In this work, we show that Flp1 is required for both fibril formation and the tenacious adherence of *A. actinomycetemcomitans*. First, immunoelectron microscopy of cells expressing an epitope-tagged version of the Flp1 polypeptide confirmed that this protein is associated with fibrils from *A. actinomycetemcomitans*. Non-polar null mutants of

flp-1 were then isolated by transposon mutagenesis and found to be defective in adherence and the ability to produce fibrils. In addition, we noted that alteration of the C-terminus of Flp1 affects the degree of adherence of *A. actinomycetemcomitans and* the ability of pili to form long, bundled arrays. Extensive phylogenetic analysis also revealed that the *flp-1* gene of *A. actinomycetemcomitans* characterizes a distinct *flp* subfamily of type IVB prepilin genes that are widespread among diverse bacterial species. Several genomes were found to code for multiple *flp* alleles and, in *A. actinomycetemcomitans*, a second allele (*flp-2*) was found immediately downstream of *flp-1*. Our results support the proposal that Flp1 is the major structural component of *A. actinomycetemcomitans* fibrils (Inoue *et al*., 1998) and also demonstrate the importance of Flp1 in fibril structure and function. In addition, the genes of the *flp* subfamily are distributed among a wide range of bacterial genomes, indicating that Flp pili may be important to the colonization properties of diverse bacterial species.

Examination of fibrils by high-resolution transmission electron microscopy showed the diameters of individual fibrils to be 5–7 nm, which is consistent with previous measurements (Rosan *et al*., 1988; Inoue *et al*., 1998) and similar to the diameters of type 1 and type IV pili (Soto and Hultgren, 1999). The electron micrographs suggested that individual pili consist of helical assemblies of subunits, presumably Flp. The putative helical structure is not surprising, as many bacterial pili display similar structures (Soto and Hultgren, 1999). The appearance of the long, bundled Flp pili of *A. actinomycetemcomitans* is strikingly similar to that of Hrp-dependent pili of *Ralstonia solanacearum* (Van Gijsegem *et al*., 2000) and the filamentous CTX phage of *V. cholerae* (Waldor and Mekalanos, 1996), even though the subunit proteins appear to be unrelated. Higher resolution techniques, such as metal shadowing, scanning transmission electron microscopy (STEM) and X-ray crystallography, will be required to confirm the helical structure of *A. actinomycetemcomitans* fibrils.

Extensive database searches revealed 20 open reading frames (ORFs) whose predicted products show high similarity to the *A. actinomycetemcomitans* Flp1 protein. These ORFs are distributed in a diverse array of bacteria. In addition, Flp1 appeared to share conserved sequence features with known type IV prepilin genes. To understand the evolutionary relationships between *flp*-like ORFs and other genes for type IV pilin subunits, we used a parsimony-based algorithm to infer pilin gene phylogeny.

Previously identified type IV prepilins and members of the *flp* gene subfamily are unified by several structural characteristics. All have the three-domain structure comprising a positively charged N-terminal leader sequence followed by a region of approximately 20 hydrophobic amino acids and a C-terminal variable region (Fig. 9). A glycine residue is invariably conserved immediately preceding the cleavage site between the leader sequence and the hydrophobic domain. With the exception of *Salmonella* spp. PilS proteins, a conserved glutamate residue is located approximately five amino acid residues after the cleavage site.

Previous reports have divided type IV prepilins into classes A and B (Strom and Lory, 1993; Skerker and Shapiro, 2000). Type IVA prepilin proteins are generally typified by a short basic leader sequence. In addition, a conserved phenylalanine residue immediately follows the cleavage site. Type IVB prepilins are characterized by longer leader peptides and the absence of phenylalanine in the position immediately after the conserved leader peptide cleavage point. Our phylogeny shows that type IVA prepilin genes form a distinct monophyletic group, and those belonging to type IVB are monophyletic only when *E. coli bfpA* is excluded from this group.

Within the type IVB family, there is a clear monophyletic *flp* subfamily. Members of this subfamily can be distinguished by several characteristics. (i) A tyrosine residue immediately follows the conserved glutamate residue in the hydrophobic domain. (ii) *flp* subfamily products are much smaller than other type IV prepilins. They conserve the three-domain structure, but the variable C-terminal region is greatly reduced in size. (iii) In every case in which the surrounding sequence is known, *flp* genes are found near (usually upstream of) genes homologous to those of the *flp–rcp–tad* region of *A. actinomycetemcomitans* (Fig. 10; Haase *et al*., 1999; Kachlany *et al*., 2000b; P. Planet, unpublished results).

By analogy with the structure of other pilins (Sauer *et al*., 2000), it seems likely that the mature Flp1 protein in the assembled pilus is packed with the N-terminus facing the core of the pilus and the C-terminus exposed to the aqueous environment. The phenotypes of mutant JK1029, which has a transposon inserted at the 3′ end of *flp-1*, indicate that the C-terminus of Flp1 has an important role in the adherence properties of the fibrils. This mutant is predicted to express a Flp1 polypeptide in which the extreme C-terminus is altered. The strain expresses pili, but they are not bundled as much as those of the wild-type strain. In addition, the strain does not adhere to surfaces as well as the wild type. The partial dominant negativity in the presence of the wild-type *flp-1* gene indicates that this polypeptide is assembled into the fibrils. These results are consistent with those of the Flp1-T7 fusion protein, which is extended at its C-terminus by the 11-amino-acid T7-TAG epitope. The Flp1-T7 polypeptide is expressed upon induction with IPTG and, because Flp1-T7 was localized to assembled fibrils, the T7-TAG did not block the processing or secretion of Flp1. However, the gene encoding Flp1-T7 was able only partially to complement the *flp-1* null mutations of JK1009 and JK1010, and it displayed a

partial dominant-negative phenotype in the wild-type strain (S. Kachlany, unpublished results). A gene fusion expressing Flp1 with the 11-amino-acid HSV epitope at its C-terminus also complemented the *flp-1* null mutants, but poorly (S. Kachlany, unpublished results). Taken together, these observations indicate that the fibril bundling and adherence properties of *A. actinomycetemcomitans* are determined by the structure of the C-terminal region of Flp1. This model predicts that chemically altering the C-terminus of Flp1 would alter or inhibit the adherence of *A. actinomycetemcomitans*.

The phylogeny of the *flp* subfamily reveals an evolutionary tendency to conserve duplicated *flp* genes. The *flp* genes of *C. tepidum*, *Chlorobium limicola* and *H. ducreyi* appear to have duplicated recently within these species, as each *flp* gene is most closely related to the other *flp* genes from the same species. Other events, such as the duplication of *flp* into *A. actinomycetemcomitans flp-1* and *flp-2*, seem to have occurred in an ancestor of this genetic locus because *flp-1* from *A. actinomycetemcomitans* is most closely related to *flp-1* of *P. multocida*, not to *flp-2* of *A. actinomycetemcomitans.* These duplication patterns reveal the creation of paralogous gene groupings both within extant species and in common ancestors. Thorough sampling of closely related *flp* genes will allow a more accurate inference of the historical pattern of duplication.

At present, it is not known why multiple alleles are so common in the *flp* subfamily. Duplicated *flp* prepilin genes may play slightly different structural roles, be expressed in different contexts, act as regulatory elements or merely increase production of pilin subunits by increasing gene dose. The multiple alleles of *flp* may allow interactions of cells with different surfaces. Pathogens may differentially express *flp* alleles for antigenic variation or host adaptation. Because *flp* homologues are found in several disease-causing bacteria, understanding Flp structure, function and phylogeny may provide exciting possibilities for the development of vaccines and chemotherapeutic interventions that inhibit the binding of pathogens to host surfaces.

Experimental procedures

Bacterial strains and growth conditions

A. actinomycetemcomitans strains used in this study are described in Table 1. *A. actinomycetemcomitans* CU1000N is a nalidixic acid-resistant variant of the adherent clinical isolate, CU1000, which has been described previously (Fine *et al*., 1999a, b; Kachlany *et al*., 2000b). *A. actinomycetemcomitans* strains were grown in AAGM (Fine *et al*., 1999b) using the following antibiotic concentrations where appropriate: chloramphenicol (Cm), 4 μg ml^{-1}; kanamycin (Km), 40 μg ml^{-1}; nalidixic acid, 20 μg ml^{-1}. *Escherichia coli* strain TOP10 (Invitrogen), used as the conjugative donor to mobilize plasmids to *A. actinomycetemcomitans*, was grown in Luria–Bertani (LB) broth and on LB agar (Miller, 1972) with chloramphenicol (50 μg ml^{-1}) or kanamycin (50 μg ml^{-1}), where appropriate. The method for mobilization using the RK2 *oriT*-defective mutant plasmid, pRK21761, has been described previously (Thomson *et al*., 1999). For genetic complementation studies and immunogold localization of Flp1-T7, *A. actinomycetemcomitans* strains carrying the appropriate *tacp* expression plasmid were grown in the presence of 1.0 mM IPTG.

DNA procedures and plasmid constructions

The plasmids used in this study are shown in Table 1. The nucleotide sequence of the *flp-1*/*flp-2* region of CU1000N was determined multiple times using different combinations of flanking oligonucleotide primers to amplify the region by PCR (Saiki *et al*., 1988). The nucleotide sequences of the PCR products were done by the Columbia University DNA Sequencing Facility using a Perkin-Elmer Applied Biosystems automated DNA sequencer 373A. The nucleotide sequence was confirmed for both strands, and the sequence was deposited into GenBank under accession number AF320002. The plasmid containing the wild-type *flp-1* gene from CU1000N (pRA33) was constructed as follows. First, the *flp-1* gene was amplified using the primers 5′-AACAACAATAGGAGCATTAAGACA-3′ (flpUP) and 5′-GTATTTAATATTTAAGTTGTTACTTATT-3′ (flpDWN). This product, as well as all other PCR-generated products, was cloned into pCR2.1 TOPO (Invitrogen). For expression of genes in *A. actinomycetemcomitans*, products were further cloned into pJAK16 using standard cloning procedures as described previously (Kachlany *et al*., 2000b). The plasmid used for the expression of Flp1-T7(pSK163) was constructed in the same manner as pRA33, except that the downstream primer (flp-T7) was 5′-TTAACCCATTTGCTGTCCACCAGTCATGCTAGCCATCTTAGTGACATTTGCACTGTAC-3′, which includes the coding sequence for the 11-amino-acid T7-TAG.

*IS*903φkan *mutagenesis of* A. actinomycetemcomitans

CU1000N carrying the IS*903*φ*kan* transposon vector, pVJT128, was grown in the presence of 2.0 mM IPTG to induce transposition, as described previously (Kachlany *et al*., 2000b). Kanamycin-resistant colonies showing a smooth morphology were characterized further. The following primers were used for PCR to screen the mutants for an insertion in the *flp* gene: FLP2 (5′-CAAACTCAAGGATTCTTG-3′) and FLP4 (5′-CCGAGAACTGCACAGCATATC-3′). These primers flank the *flp-1* region and yield a 2.0 kb PCR product, unless IS*903*φ*kan* has inserted in the region. The insertion sites were determined after amplification by inverse PCR using primers kanStart and kanStop, as described previously (Thomson *et al*., 1999). The products were cloned into plasmid LITMUS28 (New England Biolabs) and sequenced using universal primers.

Transmission electron microscopy

For the visualization of bacterial cells and Flp1-containing fibrils, we used a Jeol 1200EX transmission electron

microscope operating at 80.0 kV. Cells were first scraped from solid medium and resuspended in 0.1 ml of 10 mM Tris-HCl buffer (pH 7.5). This suspension was allowed to settle onto a Formvar carbon-coated copper grid of mesh size 200 (EM Sciences) for ≈ 10 min. The grid was immersed in 0.1 ml of filtered 1% uranyl acetate for ≈ 1 s. The grid was quickly removed, and the excess stain was wicked away with filter paper. All grids were stored in the dark in a desiccator until they were viewed, which occurred within 1 day of their preparation. Image analysis of fibrils was performed by altering the contrast so that differences were more apparent.

Immunogold electron microscopy

For the identification of Flp1-T7 in *A. actinomycetemcomitans* fibrils, strain AA1649 was grown on solid AAGM containing Cm and 1.0 mM IPTG. Cells were scraped and resuspended in an Eppendorf tube containing 50 μl of 10 mM Tris-HCl (pH 7.5), 1% BSA (wash buffer). Then, 0.5 μl of the primary anti-T7-TAG monoclonal antibody (Novagen) was added to this suspension. The tube was incubated for 30 min at 37°C and centrifuged for 1 min at 16 000 *g* to pellet cells. The supernatant was removed, 100 μl of fresh wash buffer was added, and the cells were resuspended by gentle vortex mixing. This was repeated with fresh wash buffer to remove unbound primary antibody. After the second wash, cells were resuspended in 50 μl of wash buffer containing 2.5 μl of the secondary anti-mouse, 10-nm-gold-conjugated antibody (Sigma) and incubated for 30 min at 37°C. The cells were then washed twice as before, and then twice in 10 mM Tris-HCl (pH 7.5) buffer without BSA. The cells were resuspended in 100 μl of 10 mM Tris-HCl, then added to an electron microscope grid and stained as described above.

Adherence assay

Adherence was assayed according to a modification of the protocol of O'Toole and Kolter (1998). A total of 10^5 colony-forming units (cfu) of each strain was spread onto the surface of a 100 mm Petri dish containing AAGM and grown for 18 h at 37°C in 10% CO_2. The colonies were scraped into 5 ml of fresh medium and homogenized with five strokes in a Tenbroeck tissue grinder (Wheaton). Serial decimal dilutions of cells (100 μl in triplicate) were transferred to the wells of a 96-well, flat-bottom, tissue culture-treated, polystyrene microtitre plate (Falcon 3072) and incubated for 1 h at 37°C in 10% CO_2. The wells were washed three times with 400 μl of phosphate-buffered saline (PBS) to remove loosely adherent cells and then stained with 40 μl of 0.1% crystal violet for 10 min at 37°C. Wells were washed three more times with PBS, and 100 μl of 100% ethanol was added to each well to solubilize the crystal violet. The absorbance in each well was measured at 540 nm in a Bio-Rad model 3550-UV microplate reader.

Sequence similarity searching

Nucleotide sequences similar to *flp-1* and other type IV prepilin genes were identified using the BLAST alignment program (Altschul *et al*., 1997) to search GenBank and the Microbial Finished and Unfinished Genome Databases (http://www.ncbi.nlm.nih.gov/BLAST/unfinishedgenome.html). Default settings of the BLAST program were used, except for the low-complexity filter, as this option often excluded the large N-terminal hydrophobic region from similarity and identity calculations. We excluded sequences from unfinished genomes in which the ORF was within 100 bp of the end of contig. All 61 sequences included in the analysis (Fig. 8) significantly exceeded BLAST default criteria. Two sequences from the *Bacillus anthracis* virulence plasmid pXO1 (pXO163 and pXO164), whose translated polypeptide products had significant similarity to Flp1, were excluded because these sequences were extremely labile to different alignment parameters. We retained the names of previously identified sequences obtained from searches of GenBank or any finished annotated genomes. We named unnamed ORFs in unfinished genomes from the phylogenetic analysis using the name of the smallest subfamily or clear subgrouping to which that sequence belonged.

Preliminary sequence data for *Acidithiobacillus ferrooxidans*, *C. crescentus* and *C. tepidum* were obtained from The Institute for Genomic Research at http://www.tigr.org. *Bordetella pertussis* and *Bordetella bronchiseptica* sequences were produced by the respective Sanger Centre sequencing groups (http://www.sanger.ac.uk/); *A. actinomycetemcomitans* by the University of Oklahoma's Advanced Center for Genome Technology (http://www.genome.ou.edu); *H. ducreyi* (http://www.htsc.washington.edu/hducreyi/info/index.cfm); *Sinorhizobium meliloti* by Stanford University (http://cmgm.stanford.edu/~mbarnett/genome.html); *P. aeruginosa* sequence by the *Pseudomonas* Genome Project (http://www.pseudomonas.com); and the *P. multocida* sequence by the University of Minnesota *P. multocida* Genome Project (http://www.cbc.umn.edu/ResearchProjects/AGAC/Pm/index.html).

Alignment

CLUSTAL X 1.63 (Thompson *et al*., 1997) was used to align all 61 prepilin subunit amino acid sequences with a gap/change cost of 10. This alignment was then used as a template to align each prepilin DNA sequence. Both the nucleotide and the amino acid sequences were then combined into a single data matrix for phylogenetic analysis. Combination of DNA and amino acid alignments allows efficient extraction of as much sequence data as possible, while also differentially weighting codons and codon positions in the phylogenetic analysis (Agosti *et al*., 1995). The alignment is available at http://cpmcnet.columbia.edu/dept/figurski.

Phylogenetic and sequence analysis

The combined DNA and amino acid matrix was then analysed using parsimony algorithms of PAUP*4.0 (Swofford, 1998). We performed an aggressive heuristic search with 10 000 replicates of the random addition followed by the subtree pruning and regrafting (SPR) function of PAUP, saving only one tree at each replicate. All characters and state transformations were given equal weight, and gaps were treated as missing data. The resulting 3020 trees (ranging from 10 626 to 10 696 steps in length) were tested with the more rigorous tree-branch reconnection (TBR) technique.

This yielded a single most parsimonious tree of 10 626 steps. The tree was rooted using all three sequences with similarity to type IV prepilins (HofG-1, HofG-2 and HofG-3) present in the fully sequenced cyanobacterium *Synechocystis* PCC6308. Cyanobacteria are considered to be basal taxa to all other bacterial taxa represented in the phylogeny. We used the program AUTODECAY in conjunction with PAUP to calculate Bremer supports of confidence for nodes in the tree (Eriksson, 1997). Bremer decay indices represent the number of additional evolutionary steps that are required to lose the groupings represented by the phylogeny (Bremer, 1995). One hundred TBR replicates were made at each node in the phylogeny to obtain the Bremer decay index. We also calculated bootstrap supports using PAUP to perform 100 bootstrap replicates with a heuristic search using 100 random addition steps followed by TBR testing. Groups with a bootstrap score of 50% or higher are noted on the tree.

Acknowledgements

We thank Randy Aussenberg for constructing pRA33, A.-J. Silverman for helpful advice on electron microscopy, and M. Bhattacharjee, H. Schreiner and D. Furgang for their comments. We are grateful to Bruce Roe, Fares Z. Najar, Sandy Clifton, Tom Ducey, Lisa Lewis and Dave Dyer for the use of unpublished nucleotide sequence data from the *A. actinomycetemcomitans* Genome Sequencing Project at the University of Oklahoma. This work was supported in part by NIH research grants (to D. H. Figurski and D. H. Fine) and NIH traineeships (to S.C.K. and P.J.P.).

References

Agosti, D., Jacobs, D., and DeSalle, R. (1995) On combining protein sequences and nucleic acid sequences in phylogenetic analysis: the homeobox protein case. *Cladistics* **12**: 65–82.

Altschul, S.F., Madden, T.L., Schaffer, A.A., Zhang, J., Zhang, Z., Miller, W., and Lipman, D.J. (1997) Gapped BLAST and PSI-BLAST: a new generation of protein database search programs. *Nucleic Acids Res* **25**: 3389–3402.

Bremer, K. (1995) Branch support and tree stability. *Cladistics* **10**: 295–304.

Conway, B., and Ronald, A. (1988) An overview of some mechanisms of bacterial pathogenesis. *Can J Microbiol* **34**: 281–286.

Costerton, J.W., Lewandowski, Z., Caldwell, D.E., Korber, D.R., and Lappin-Scott, H.M. (1995) Microbial biofilms. *Annu Rev Microbiol* **49**: 711–745.

Eriksson, T. (1997) *Autodecay*. Hypercard stack distributed by the author, Botaniska instiutionen, Stockholm University: Stockholm.

Felsenstein, J. (1985) Confidence limits on phylogenies: an approach using the bootstrap. *Evolution* **39**: 783–791.

Fine, D.H., Furgang, D., Kaplan, J., Charlesworth, J., and Figurski, D.H. (1999a) Tenacious adhesion of *Actinobacillus actinomycetemcomitans* strain CU1000 to salivary-coated hydroxyapatite. *Arch Oral Biol* **44**: 1063–1076.

Fine, D.H., Furgang, D., Schreiner, H.C., Goncharoff, P., Charlesworth, J., Ghazwan, G., *et al.* (1999b) Phenotypic variation in *Actinobacillus actinomycetemcomitans* during laboratory growth: implications for virulence. *Microbiology* **145**: 1335–1347.

Finlay, B.B., and Falkow, S. (1997) Common themes in microbial pathogenicity revisited. *Microbiol Mol Biol Rev* **61**: 136–169.

Fives-Taylor, P.M., Meyer, D.H., Mintz, K.P., and Brissette, C. (2000) Virulence factors of *Actinobacillus actinomycetemcomitans*. *Periodontology* **20**: 136–167.

Graber, K.R., Smoot, L.M., and Actis, L.A. (1998) Expression of iron binding proteins and hemin binding activity in the dental pathogen *Actinobacillus actinomycetemcomitans*. *FEMS Microbiol Lett* **163**: 135–142.

Haase, E.M., Zmuda, J.L., and Scannapieco, F.A. (1999) Identification and molecular analysis of rough-colony-specific outer membrane proteins of *Actinobacillus actinomycetemcomitans*. *Infect Immun* **67**: 2901–2908.

Hacker, J. (1992) Role of fimbrial adhesins in the pathogenesis of *Escherichia coli* infections. *Can J Microbiol* **38**: 720–727.

Harano, K., Yamanaka, A., and Okuda, K. (1995) An antiserum to a synthetic fimbrial peptide of *Actinobacillus actinomycetemcomitans* blocked adhesion of the microorganism. *FEMS Microbiol Lett* **130**: 279–285.

Holt, S.C., Tanner, A.C., and Socransky, S.S. (1980) Morphology and ultrastructure of oral strains of *Actinobacillus actinomycetemcomitans* and *Haemophilus aphrophilus*. *Infect Immun* **30**: 588–600.

Inoue, T., Tanimoto, I., Ohta, H., Kato, K., Murayama, Y., and Fukui, K. (1998) Molecular characterization of low-molecular-weight component protein, Flp, in *Actinobacillus actinomycetemcomitans* fimbriae. *Microbiol Immunol 42*: 253–258.

Inoue, T., Ohta, H., Tanimoto, I., Shingaki, R., and Fukui, K. (2000) Heterogeneous post-translational modification of *Actinobacillus actinomycetemcomitans* fimbrillin. *Microbiol Immunol* **44**: 715–718.

Inouye, T., Ohta, H., Kokeguchi, S., Fukui, K., and Kato, K. (1990) Colonial variation and fimbriation of *Actinobacillus actinomycetemcomitans*. *FEMS Microbiol Lett* **57**: 13–17.

Ishihara, K., Honma, K., Miura, T., Kato, T., and Okuda, K. (1997) Cloning and sequence analysis of the fimbriae associated protein (fap) gene from *Actinobacillus actinomycetemcomitans*. *Microb Pathog* **23**: 63–69.

Kachlany, S.C., Fine, D.H., and Figurski, D.H. (2000a) Secretion of RTX leukotoxin by *Actinobacillus actinomycetemcomitans*. *Infect Immun* **68**: 6094–6100.

Kachlany, S.C., Planet, P.J., Bhattacharjee, M.K., Kollia, E., DeSalle, R., Fine, D.H., and Figurski, D.H. (2000b) Nonspecific adherence by *Actinobacillus actinomycetemcomitans* requires genes widespread in bacteria and archaea. *J Bacteriol* **182**: 6169–6176.

Klemm, P. (1994) *Fimbriae: Adhesion, Genetics, Biogenesis, and Vaccines*. Boca Raton, FL: CRC Press, p. 283.

Kolodrubetz, D., Dailey, T., Ebersole, J., and Kraig, E. (1989) Cloning and expression of the leukotoxin gene from *Actinobacillus actinomycetemcomitans*. *Infect Immun* **57**: 1465–1469.

Lally, E.T., Kieba, I.R., Demuth, D.R., Rosenbloom, J., Golub, E.E., Taichman, N.S., and Gibson, C.W. (1989) Identification and expression of the *Actinobacillus*

actinomycetemcomitans leukotoxin gene. *Biochem Biophys Res Commun* **159**: 256–262.

Meyer, D.H., and Fives-Taylor, P.M. (1998) Oral pathogens: from dental plaque to cardiac disease. *Curr Opin Microbiol* **1**: 88–95.

Miller, J.H., and Cold Spring Harbor Laboratory (1972) *Experiments in Molecular Genetics*. Cold Spring Harbor, NY: Cold Spring Harbor Laboratory Press, p. 466.

O'Toole, G.A., and Kolter, R. (1998) Initiation of biofilm formation in *Pseudomonas fluorescens* WCS365 proceeds via multiple, convergent signalling pathways: a genetic analysis. *Mol Microbiol* **28**: 449–461.

Rosan, B., Slots, J., Lamont, R.J., Listgarten, M.A., and Nelson, G.M. (1988) *Actinobacillus actinomycetemcomitans* fimbriae. *Oral Microbiol Immunol* **3**: 58–63.

Saiki, R.K., Gelfand, D.H., Stoffel, S., Scharf, S.J., Higuchi, R., Horn, G.T., *et al.* (1988) Primer-directed enzymatic amplification of DNA with a thermostable DNA polymerase. *Science* **239**: 487–491.

Sauer, F.G., Mulvey, M.A., Schilling, J.D., Martinez, J.J., and Hultgren, S.J. (2000) Bacterial pili: molecular mechanisms of pathogenesis. *Curr Opin Microbiol* **3**: 65–72.

Scannapieco, F.A., Millar, S.J., Reynolds, H.S., Zambon, J.J., and Levine, M.J. (1987) Effect of anaerobiosis on the surface ultrastructure and surface proteins of *Actinobacillus actinomycetemcomitans* (*Haemophilus actinomycetemcomitans*). *Infect Immun* **55**: 2320–2323.

Shenker, B.J., McKay, T., Datar, S., Miller, M., Chowhan, R., and Demuth, D. (1999) *Actinobacillus actinomycetemcomitans* immunosuppressive protein is a member of the family of cytolethal distending toxins capable of causing a G2 arrest in human T cells. *J Immunol* **162**: 4773–4780.

Skerker, J.M., and Shapiro, L. (2000) Identification and cell cycle control of a novel pilus system in *Caulobacter crescentus*. *EMBO J* **19**: 3223–3234.

Slots, J., and Ting, M. (1999) *Actinobacillus actinomycetemcomitans* and *Porphyromonas gingivalis* in human periodontal disease: occurrence and treatment. *Periodontology* **20**: 82–121.

Soto, G.E., and Hultgren, S.J. (1999) Bacterial adhesins: common themes and variations in architecture and assembly. *J Bacteriol* **181**: 1059–1071.

Sprunt, K., and Leidy, G. (1988) The use of bacterial interference to prevent infection. *Can J Microbiol* **34**: 332–338.

Strom, M.S., and Lory, S. (1993) Structure–function and biogenesis of the type IV pili. *Annu Rev Microbiol* **47**: 565–596.

Sun, D.X., Mekalanos, J.J., and Taylor, R.K. (1990) Antibodies directed against the toxin-coregulated pilus isolated from *Vibrio cholerae* provide protection in the infant mouse experimental cholera model. *J Infect Dis* **161**: 1231–1236.

Thompson, J.D., Higgins, D.G., and Gibson, T.J. (1997) *CLUSTAL X Multiple Sequence Alignment Program*. Hamburg, Germany: European Molecular Biology Organization.

Swofford, D.L. (1999) PAUP Version 4.02b. Sinauer Associates, Inc. Publishers.

Thomson, V.J., Bhattacharjee, M.K., Fine, D.H., Derbyshire, K.M., and Figurski, D.H. (1999) Direct selection of IS903 transposon insertions by use of a broad-host-range vector: isolation of catalase-deficient mutants of *Actinobacillus actinomycetemcomitans*. *J Bacteriol* **181**: 7298–7307.

Van Gijsegem, F., Vasse, J., Camus, J.C., Marenda, M., and Boucher, C. (2000) *Ralstonia solanacearum* produces hrp-dependent pili that are required for PopA secretion but not for attachment of bacteria to plant cells. *Mol Microbiol* **36**: 249–260.

Waldor, M.K., and Mekalanos, J.J. (1996) Lysogenic conversion by a filamentous phage encoding cholera toxin. *Science* **272**: 1910–1914.

Wizemann, T.M., Adamou, J.E., and Langermann, S. (1999) Adhesins as targets for vaccine development. *Emerg Infect Dis* **5**: 395–403.